

## Damping and frequency of twin-cables with a cross-link and a viscous damper

H.J. Zhou<sup>1,2a</sup>, X. Yang<sup>1b</sup>, Y.R. Peng<sup>1c</sup>, R. Zhou<sup>\*1</sup>, L.M. Sun<sup>3d</sup> and F. Xing<sup>2e</sup>

<sup>1</sup>Institute of Urban Smart Transportation & Safety Maintenance, Shenzhen University, Nanhai Ave 3688, Shenzhen 518060, China

<sup>2</sup>Guangdong Provincial Key Laboratory of Durability for Marine Civil Engineering, Shenzhen University, Nanhai Road 3688, Shenzhen, Guangdong 518060, P.R. China

<sup>3</sup>State Key Laboratory for Disaster Reduction in Civil Engineering, Tongji University, Siping Road 1239, Shanghai 200092, P.R. China

(Received August 25, 2018, Revised January 18, 2019, Accepted January 25, 2019)

**Abstract.** Vibration mitigation of cables or hangers is one of the crucial problems for cable supported bridges. Previous research focused on the behaviors of cable with dampers or cross-ties, which could help engineering community apply these mitigation devices more efficiently. However, less studies are available for hybrid applied cross-ties and dampers, especially lack of both analytical and experimental verifications. This paper studied damping and frequency of two parallel identical cables with a connection cross-tie and an attached damper. The characteristic equation of system was derived based on transfer matrix method. The complex characteristic equation was numerically solved to find the solutions. Effects of non-dimensional spring stiffness and location on the maximum cable damping, the corresponding optimum damper constant and the corresponding frequency of lower vibration mode were further addressed. System with twin small-scale cables with a cross-link and a viscous damper were tested. The damping and frequency from the test were very close to the analytical ones. The two branches of solutions: in-phase modes and the out-of-phase modes, were identified; and the two branches of solutions were different for damping and frequency behaviors.

**Keywords:** cable; cross-link; damper; damping; frequency

### 1. Introduction

Cables and hangers are vulnerable to wind or wind/rain excitations (Hikami and Shiraishi, 1988; Gjelstrup, et al., 2007; Xu, et al., 2008) as they are slender structures with low damping and frequency characteristics. Large amplitude cable vibration was occasionally reported and sometimes adjacent cables would collide with each other. Recognizing the severe danger posed by hanger/cable vibrations, researchers have investigated three different ways to solve this problem: aerodynamic counter-measures (Gu and Du 2005, Zhan *et al.* 2008), installing passive/semi-active dampers (Fujino *et al.* 1993, Krenk 2000, Main and Jones 2001, Sun *et al.* 2004, Chen *et al.*

2004, Duan *et al.* 2005, 2006 2019a, b, Wang *et al.* 2005, Christenson *et al.* 2006, Zhou, *et al.*, 2006 and 2014b; Or, et al., 2008; Zhou and Sun 2008, 2013, Lu *et al.* 2017) and connecting adjacent cables by cross-ties (Yamaguchi and Nagahawatta 1995, Caracoglia and Jones 2005).

The above methods have been applied in engineering practices (Chen *et al.* 2004), and full-scale test had tested the damping effects of dampers (Zhou *et al.* 2014b, 2018c). Recent investigations were focused on further improvement of damping efficiency (Xiang *et al.* 2016, Zhou and Li 2016, Zhou *et al.* 2018a, c). Another topic was connecting cables with cross-ties (Sun *et al.* 2007, Ahmad *et al.* 2016, Zhou *et al.* 2018b), especially hybrid application of both cross-ties and dampers (Bosch and Park, 2005; Sun, et al., 2005; Zhou, *et al.*, 2014a, 2015). Cross-ties and dampers were hybrid applied in some bridges as both frequency and modal damping could be added. Caracoglia and Jones (2007) reported the cable-network-damper system applied in the Fred Hartman Bridges; Caracoglia and Zuo (2009) further studied this system for possible mitigation applications. However, the dynamics and the system parameter optimization of the hybrid mitigation system still needs further investigation; and little experimental studies on hybrid mitigation of modal cables were available for the best of author's collection.

Recently, Zhou *et al.* (2015) proposed a hybrid mitigation system of two cables with a cross-ties and near support dampers. In this following paper, the analytical

\*Corresponding author, Assistant Professor

E-mail: zhourui@szu.edu.cn

<sup>a</sup>Professor

E-mail: haijun@szu.edu.cn

<sup>b</sup>Research Assistant

E-mail: yb871211@126.com

<sup>c</sup>Research Assistant

E-mail: SZPYR@outlook.com

<sup>d</sup>Professor

E-mail: lmsun@tongji.edu.cn

<sup>e</sup>Professor

E-mail: xingf@szu.edu.cn

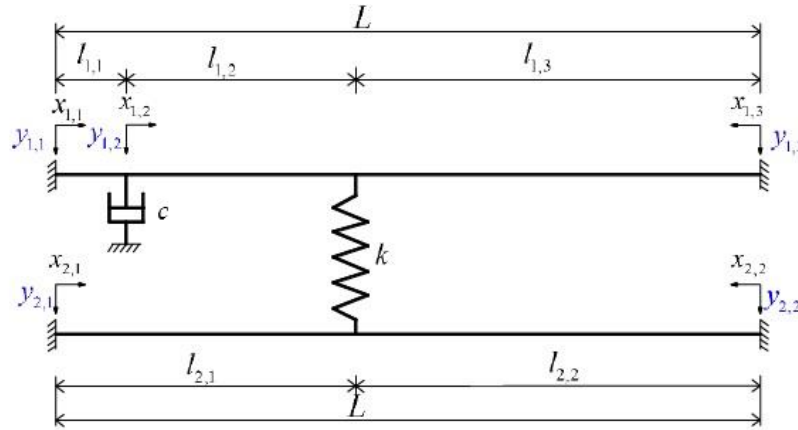


Fig. 1 Two identical cables with a connection cross-link and a viscous damper

model of two identical cables (twin-cables) connected with a cross-link and an attached damper was developed. This kind of system was widely applied in hangers of suspension or arch bridges; and it is a special kind of the hybrid mitigation system. The frequency equation of the system was derived. An experimental test was further carried out with two small scale cables with a connecting cross-link and calibrated dampers; comparison of test damping and frequency of the system to analytical solutions was made.

**2. Characteristic equation**

Fig.1 shows two identical cables (twin-cables) are interconnected by a vertical cross-link and a damper, without loss of generality, the damper is located near to the left anchorage of the first (upper) cable. The influence of cables' weight on tension force is neglected as it is small compared to cable tension force. The geometric and physical characteristic of the cable are indicated as: length  $L$ , tension force  $T$ , mass per unit length  $m$ . The damping coefficient of the damper is  $c$ . The axial stiffness of the cross-link is  $k$ . The length of the  $P_j$  segment of the  $j^{th}$  cable is  $l_{j,p_j}$  ( $p_1=1,2,3$  and  $p_2=1,2$ ) and its axial coordinate is  $x_{j,p_j}$ .

The linearized motion equation of each cable segment is (Irvine 1981)

$$m \frac{\partial^2 y_{j,p_j}(x_{j,p_j}, t)}{\partial t^2} = T \frac{\partial^2 y_{j,p_j}(x_{j,p_j}, t)}{\partial x_{j,p_j}^2} \tag{1}$$

where  $y_{j,p_j}(x_{j,p_j}, t)$  is the transverse displacement of each cable segment, which can be expressed as

$$y_{j,p}(x_{j,p}, t) = Y_{j,p_j}(x_{j,p_j}) e^{\lambda \tau} \tag{2}$$

where  $Y_{j,p_j}(x_{j,p_j})$  is the complex mode shape function. A non-dimensional time  $\tau = \omega_0 t$  is introduced with

$\omega_0 = \pi/L \sqrt{T/m}$  being the real fundamental circular frequency of the cable, and  $\lambda$  is a non-dimensional eigenvalue, which can be expressed in terms of real and imaginary parts as

$$\lambda = \alpha + i\beta = \frac{\omega}{\omega_0} \left( -\xi + i\sqrt{1-\xi^2} \right) \tag{3}$$

in which  $i = \sqrt{-1}$ ,  $\beta$  is the non-dimensional frequency of the system,  $\omega$  is the modulus of the system eigenvalue, and  $\xi = |\alpha|/\sqrt{\alpha^2 + \beta^2}$  is the damping ratio.

Substituting Eq. (2) into Eq. (1) yields

$$\frac{\partial^2 Y_{j,p_j}(x_{j,p_j})}{\partial x_{j,p_j}^2} = \left( \frac{\pi\lambda}{L} \right)^2 Y_{j,p_j}(x_{j,p_j}) \tag{4}$$

Considering the continuity of displacement,  $Y_{j,p}(x_{j,p})$  can be expressed as

$$Y_{j,p_j}(x_{j,p_j}) = A_{j,p_j} \frac{\sinh(\pi\lambda x_{j,p_j}/L)}{\sinh(\pi\lambda l_{j,p_j}/L)} + B_{j,p_j} \frac{\cosh(\pi\lambda x_{j,p_j}/L)}{\cosh(\pi\lambda l_{j,p_j}/L)} \tag{5}$$

where  $A_{j,p_j}$  and  $B_{j,p_j}$  are complex parameters.

Displacement boundary conditions at cable ends are

$$y_{1,1}(x_{1,1} = 0, t) = y_{1,3}(x_{1,3} = 0, t) = 0 \tag{6a}$$

$$y_{2,1}(x_{2,1} = 0, t) = y_{2,2}(x_{2,2} = 0, t) = 0 \tag{6b}$$

Displacement continuity equations at the damper and spring locations are

$$y_{1,1}(x_{1,1} = l_{1,1}, t) = y_{1,2}(x_{1,2} = 0, t) \tag{7a}$$

$$y_{1,2}(x_{1,2} = l_{1,2}, t) = y_{1,3}(x_{1,3} = l_{1,3}, t) \tag{7b}$$

$$y_{2,1}(x_{2,1} = l_{2,1}, t) = y_{2,2}(x_{2,2} = l_{2,2}, t) \tag{7c}$$

Force equilibrium equations at dampers locations and the spring location are

$$T \left( \frac{\partial y_{1,2}}{\partial x_{1,2}} \Big|_{x_{1,2}=0} - \frac{\partial y_{1,1}}{\partial x_{1,1}} \Big|_{x_{1,1}=l_{1,1}} \right) = c \frac{\partial y_{1,1}}{\partial t} \Big|_{x_{1,1}=l_{1,1}} \tag{8a}$$

$$T \left( \frac{\partial y_{1,2}}{\partial x_{1,2}} \Big|_{x_{1,2}=l_{1,2}} + \frac{\partial y_{1,3}}{\partial x_{1,3}} \Big|_{x_{1,3}=l_{1,3}} \right) = k \left( y_{2,1} \Big|_{x_{2,1}=l_{2,1}} - y_{1,2} \Big|_{x_{1,2}=l_{1,2}} \right) \tag{8b}$$

$$T \left( \frac{\partial y_{1,2}}{\partial x_{1,2}} \Big|_{x_{1,2}=l_{1,2}} + \frac{\partial y_{1,3}}{\partial x_{1,3}} \Big|_{x_{1,3}=l_{1,3}} \right) + T \left( \frac{\partial y_{2,1}}{\partial x_{2,1}} \Big|_{x_{2,1}=l_{2,1}} + \frac{\partial y_{2,2}}{\partial x_{2,2}} \Big|_{x_{2,2}=l_{2,2}} \right) = 0 \tag{8c}$$

Substituting Eqs. (2) and (5) into Eqs. (6)-(8), then Eqs. (7) and (8) can be re-written in the matrix form as

$$\mathbf{S}\Phi = \mathbf{0} \tag{9}$$

Where

$\Phi = [A_{1,1} \ A_{1,2} \ B_{1,2} \ A_{1,3} \ A_{2,1} \ A_{2,2} \ B_{2,2} \ A_{2,3}]^T$ , the sub-items of  $\Phi$  and  $\mathbf{S}$  are listed in the Appendix.

To get non-trivial solution ( $\Phi \neq \mathbf{0}$ ), the determinant of the matrix  $\mathbf{S}$  must be equal to zero. After simplifying trigonometric functions, regarding that  $l_{2,1} = l_{1,1} + l_{1,2}$  and  $l_{2,2} = l_{1,3}$ , the equation  $\det(\mathbf{S}) = 0$  can be written as

$$\lambda \sinh \Gamma \left[ \sinh \Gamma + \eta \sinh \Gamma_{1,1} \sinh (\Gamma_{1,2} + \Gamma_{1,3}) \right] + \gamma \sinh \Gamma_{1,3} \left\{ \begin{array}{l} \sinh (\Gamma_{1,1} + \Gamma_{1,2}) \\ \left[ \sinh \Gamma + \eta \sinh \Gamma_{1,1} \sinh (\Gamma_{1,2} + \Gamma_{1,3}) \right] \\ + \sinh \Gamma \\ \left[ \sinh (\Gamma_{1,1} + \Gamma_{1,2}) + \eta \sinh \Gamma_{1,1} \sinh \Gamma_{1,2} \right] \end{array} \right\} = 0 \tag{10}$$

in which  $\gamma = kL/\pi T$  is the non-dimensional spring stiffness,  $\eta = c/\sqrt{Tm}$  is the non-dimensional damper coefficient,  $\Gamma_{j,p_j} = \pi \lambda l_{j,p_j}/L$  and  $\Gamma = \pi \lambda$ .

Eq. (10) is the characteristic equation of the two identical cables with a connection cross-link and a viscous damper. It contains two parts. The first part contains two sub-equations, which are the characteristic equations of a taut cable attached with a damper (Krenk 2000, Main and Jones 2002) and a taut cable; they could be derived when there is no connection cross-tie ( $\gamma = 0$ ). The second part takes into effects of cross-links, it is the characteristic

equation of the system when the cross-tie is very rigid ( $\gamma \rightarrow \infty$ ).

For specific values of  $\gamma$ ,  $\eta$  and  $l_{j,p}/L$ , Eq. (10) can be numerically solved for  $\lambda$ , and  $\Phi$  could be obtained by substituting  $\lambda$  into Eq. (9), then the corresponding mode shape can be obtained from Eq. (5). It should be noted that Eq. (10) is a transcendental equation and has infinite solutions. The “fsolve” function in MATLAB was applied to find the solutions in this paper; and the exact target solutions were highly depended on the input initial values due to multiple mode frequencies. The initial value of frequency that near to target frequency (from analytical studies) should be selected to get the target mode frequency and damping.

### 3. Solution characteristics

#### 3.1 Two branch solutions

Previous studies (Caracoglia and Jones 2005, Ahmad and Cheng 2011) found that the characteristic equation of twin-cables with a connection cross-link has two sets of solutions: in-phase modes and out-of-phase modes; Zhou *et al.* (2015) further confirmed that the characteristic equation of twin-cables with a connection cross-link and two dampers attached to two cables still followed the above rule. For the in-phase modes, mode shapes of the two cables are in phase and similar to the mode shapes of a free cable. For the out-of-phase modes, mode shapes are out of phase and maybe dominated by some cable segments when the cross-link was very rigid. For the case of single damper attachment, studies showed that as the damper was very close to cable end, the solutions still could be classified by the two sets of in-phase and out-of-phase (Zhou *et al.* 2019), although the mode shape of the twin-cables were not exactly the same due to the fact of single damper attachment (Zhou *et al.* 2015). Fig. 2 shows the 1<sup>st</sup> to 4<sup>th</sup> mode shapes together with the corresponding  $\lambda$  values when  $l_{1,2}/L=0.2$ ,  $\gamma=10$  and  $\eta=5$ . It clearly shows the vibration mode of the system could well be distinguished by the in-phase and out-of-phase modes.

#### 3.2 Effects of spring stiffness and location

In engineering applications of the above hybrid system, the system damping and frequency is highly interested for better mitigation performance; while the parameters need to be designed are cross-link stiffness and location, damper coefficient and location. As the system frequency is mainly determined by cross-link and the system damping determined by damper coefficient, the following studied the effects of cross-link stiffness and location on system frequency, maximum attainable damping and corresponding optimum damper coefficient; and three representative values for the nondimensional cross-link stiffness: low value ( $\gamma = 1$ ), intermediate value ( $\gamma = 10$ ), and high value ( $\gamma = 50$ ) were selected for numerical solution. Without loss of generality, the damper was taken to be fixed at 2% of the

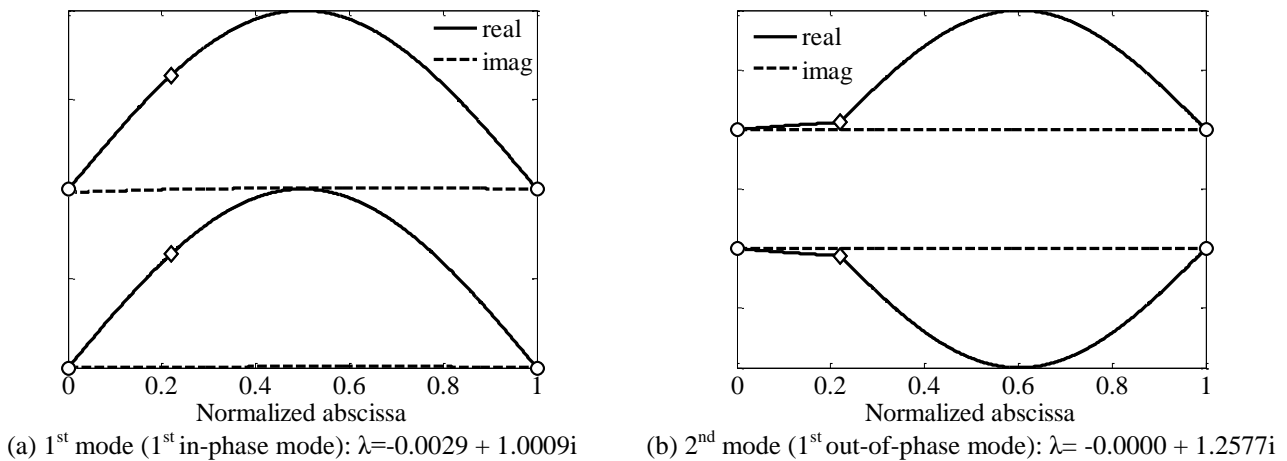


Fig. 2 Mode shapes of two identical cables with a connection cross-link and a viscous damper ( $l_{1,1}/L = 2\%$ ,  $l_{1,2}/L = 0.2$ ,  $\gamma = 10$ ,  $\eta = 5$ )

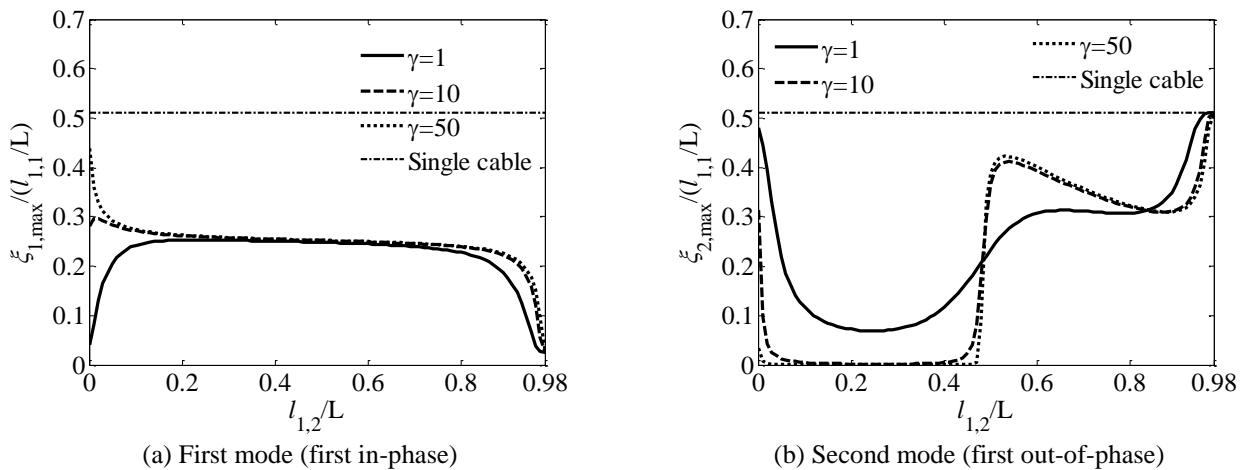


Fig. 3 Maximum damping ratio ( $l_{1,1}/L = 2\%$ )

cable length (2% to 4% in engineering applications) while the cross-link location moved along the cable axis ( $l_{1,2}/L = 0 \rightarrow 1 - l_{1,1}/L$ ).

Fig.3 shows the non-dimensional maximum damping ratio of the 1<sup>st</sup> mode (the 1<sup>st</sup> in-phase mode) and the 2<sup>nd</sup> mode (the 1<sup>st</sup> out-of-phase mode) as the cross-link moves from damper location to the right cable ends. The non-dimensional maximum damping ratio of single cable with an attached viscous damper was also shown for easy of comparison. The maximum damping ratios of the two modes are lower than that of a single cable with an attached viscous damper. It also clearly shows that the maximum damping changes significantly when cross-link was near to damper or at right cable ends as non-dimensional cross-link stiffness increases for the first in-phase mode; however, the maximum damping is almost the same for the three different non-dimensional cross-link stiffness when  $l_{1,2}/L$  is between 0.2-0.8 (Fig. 3(a)), and the maximum damping

ratio of the 1<sup>st</sup> in-phase mode  $\xi_{\max} / (l_{1,1}/L) \approx 0.25$ , which is about half of that of a single cable attached with a viscous damper ( $\xi_{\max} / (l_{1,1}/L) \approx 0.5$ , Krenk 2000). Fig. 3(b) shows that higher maximum damping ratio of the out-of-phase mode can be achieved when the cross-link is located at the right half segment of cable for  $\gamma = 10$  and 50 cases; the maximum damping ratio is very low when cross-link is located at the left half segment of cable (almost zero when  $l_{1,2}/L$  is between 0.1-0.4). The reason is due to the fact of local segment cable vibration for high cross-link stiffness, the damper would not be effective when the cable segment with attached damper does not vibrate.

Fig. 4 shows the corresponding frequency of the two modes, it shows that the vibration frequency increases as  $\gamma$  increases. However, the increment of frequency is insignificant for in-phase mode. For out-of-phase mode, the frequency is greatly increased as cross-link stiffness

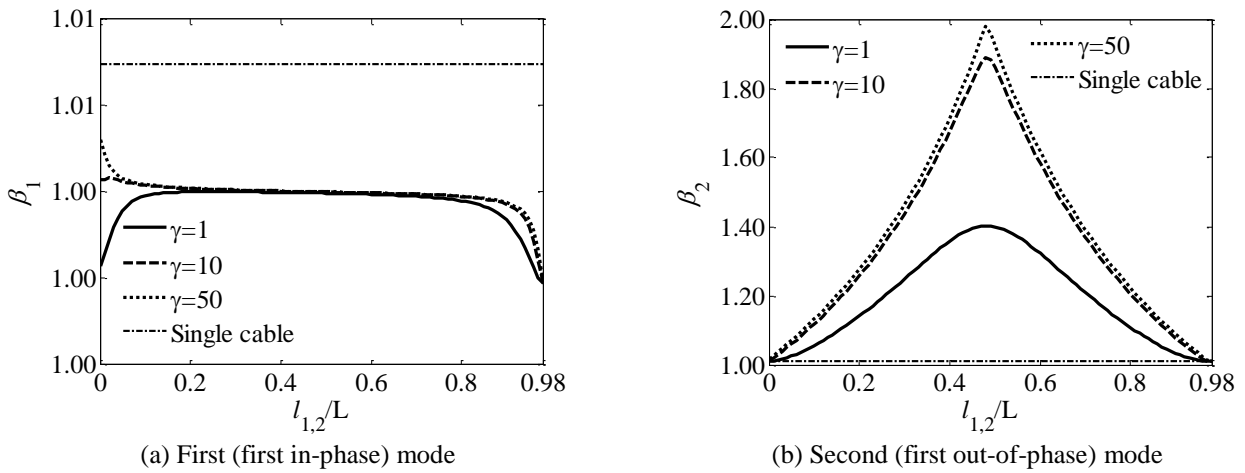


Fig. 4 Corresponding mode frequency

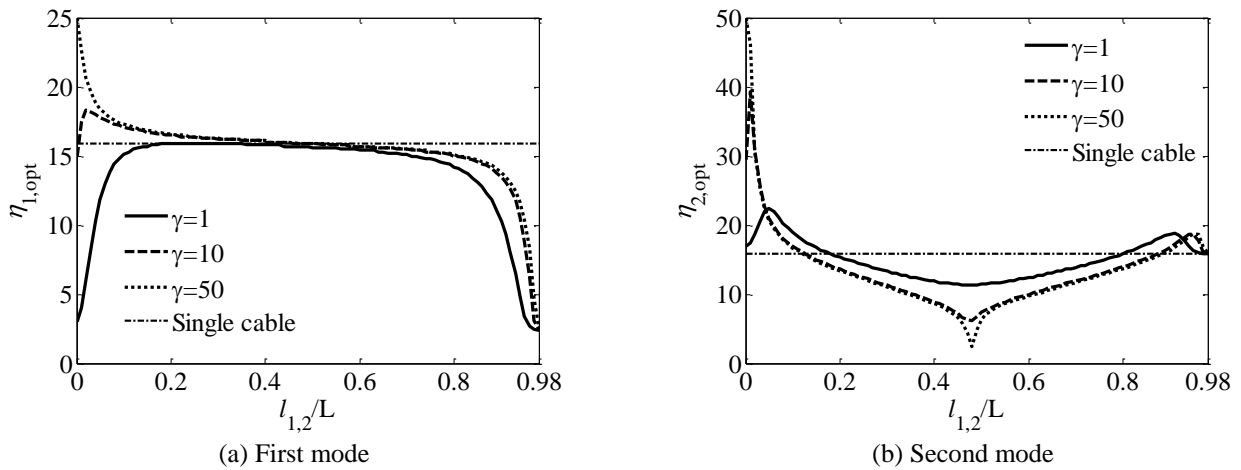


Fig. 5 Corresponding optimum damper constant ( $l_{1,1}/L = 2\%$ )

Table 1 Properties of the twin model cables

Length L (m)	Diameter (mm)	Unit Mass m (kg/m)	Inclination Angle $\theta$ ( $^\circ$ )	Initial tension T(N)	Elastic Modulus E (GPa)	Axial Rigidity EA (kN)
3.2	1.5	0.9585	22.1	600	170	300.415

increases; however, the increment of frequency from  $\gamma=10$  to  $\gamma=50$  is not so obvious as  $\gamma$  increases from 1 to 10. Together with Fig. 3, it can be concluded that the soft cross-link ( $\gamma=1$ ) have advantage of both damping and frequency improvement. The system with rigid cross-link could have higher frequency and higher damping in some cross-link locations, but rigid cross-link could also lead to local cable segment vibration without damping effects from the viscous damper.

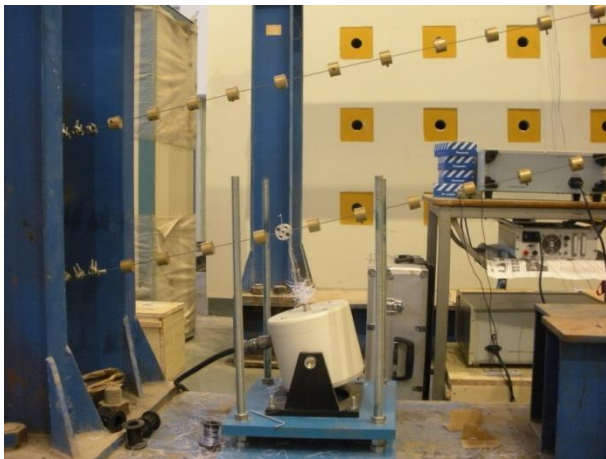
Fig. 5 further shows the corresponding non-dimensional optimum damper constant of the two modes. The optimum damper constant changes significantly when cross-link is near to damper location; however, it only changes slightly or moderately when cross-link locates at other places. It

could be concluded that the non-dimensional optimum damper constant is sensitive to the cable vibration mode number and cross-link location, but not very sensitive to the cross-link stiffness.

The previous studies of the coauthors (Zhou *et al.* 2015) showed that the system damping ratio and frequency changes regularly as the spring stiffness and locations changes, as such, no further discussion about higher mode vibration was given in this paper. The above studies showed that the damping and frequency could be both added by connecting two cables and attaching a viscous damper. In the following, experimental test was carried out to verify the above numerical results and further discuss the advantage of the proposed system.



Fig. 6 Experimental setup of small-scale twin-cable system with a viscous damper



(a) Vibration exciter



(b) Laser displacement sensor

Fig. 7 Test instruments

#### 4. Small-scale twin-cables test

##### 4.1 Experimental setup

The small-scale cable system was made up of two inclined identical cables (twin-cables), which were connected by a metal wire and the lower cable was attached with a viscous damper near to higher cable end (Fig. 6). The twin model cables were made up of two steel wires with added copper masses. The properties of the two model cables were summarized in Table 1.

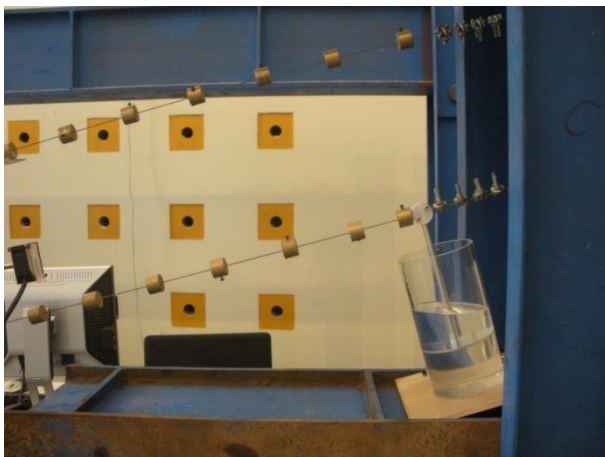
Figs. 6 and 7 shows the instruments used in the test. A vibration exciter (Fig. 7 (a)) was installed close to the lower end of the lower cable to excite the system. Four laser sensors (Fig. 7(b)) were used to record the vertical displacement of the quarter and middle point of the two cables, respectively. The cross-link locations changed from 0.1L to 0.8L with interval of 0.1L, due to the fact of very stiff cross-ties applied in cable vibration mitigation

practices, a large non-dimensional spring stiffness about 65 was used in the test.

The viscous damper was located on the lower cable by the location of 4.5%L from the cable's upper end (Fig. 8(a)). The linear viscous damper is designed and calibrated by referring to Huang (2011). It was made of a cylinder container with filled silicone oil; and an aluminum plate (Fig. 8(b)) moved in the silicone oil to generate damping force with an aluminum bar linked to the cable end. Different weights were applied on the head of the aluminum bar to let the plate drop in silicone oil (Fig. 8(c)). The displacement of the aluminum plate was measured by laser sensor. Then velocity could be derived by differential of the displacement data, and the linear damping coefficients could be derived from the F-v relation by the least square method (Fig. 8(d)). Seven different damping coefficients were derived by combining 5 different diameter aluminum plates with 2 different viscosity of silicon oils during the test (Table 2).

Table 2 Combination of seven damper coefficients

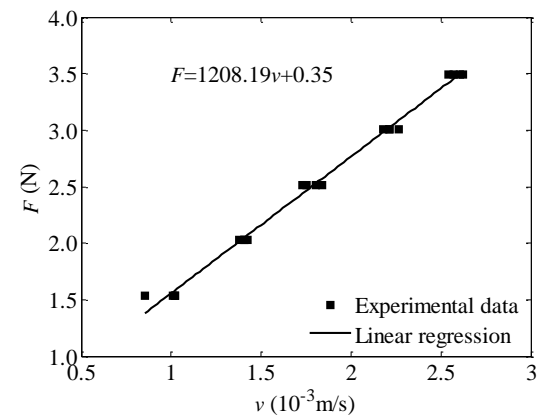
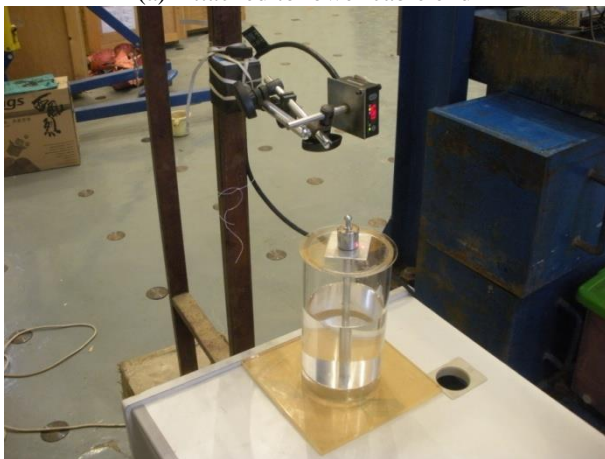
No.	Aluminum diameter (cm)	Silicon oil viscosity (mm <sup>2</sup> /s)	Damping coefficient $c$ (N·s/m)	Non-dimensional damper constant $\eta$
1	5	5000	13.16	0.54
2	6	5000	26.23	1.09
3	7	5000	49.61	2.07
4	8	5000	109.59	4.57
5	8	10000	310.86	12.96
6	9	5000	525.37	21.91
7	9	10000	1208.19	50.38



(a) Attached to lower cable end



(b) 5 aluminum plates of different diameter



(d) Calibrated force-velocity relation

Fig. 8 Viscous damper

#### 4.2 Experimental procedure and data processing

Free vibration of single cable, twin-cables with a cross-link but without viscous damper, and twin-cables with a cross-link and a viscous damper were tested. The eigen-frequency was derived by FFT analysis of the free vibration test data. Then the cable system was excited by the vibration exciter tuned at the system's eigen-frequency, after the cables reached to a steady vibration amplitude for about 20 seconds, the nylon wire connecting the cable and

the exciter was cut and the cable system vibrated in free decay. The recorded free decay displacement time-histories from laser sensors (Fig. 9(a)) were FFT analyzed (Fig. 9(b)) and then filtered by using the band pass filter in MATLAB. The mean damping ratio (Fig. 10) are obtained by using logarithmic decrement method from the filtered displacement time-histories. The test actually run twice for each case, and it was found that the two-test cases repeated well during the test.

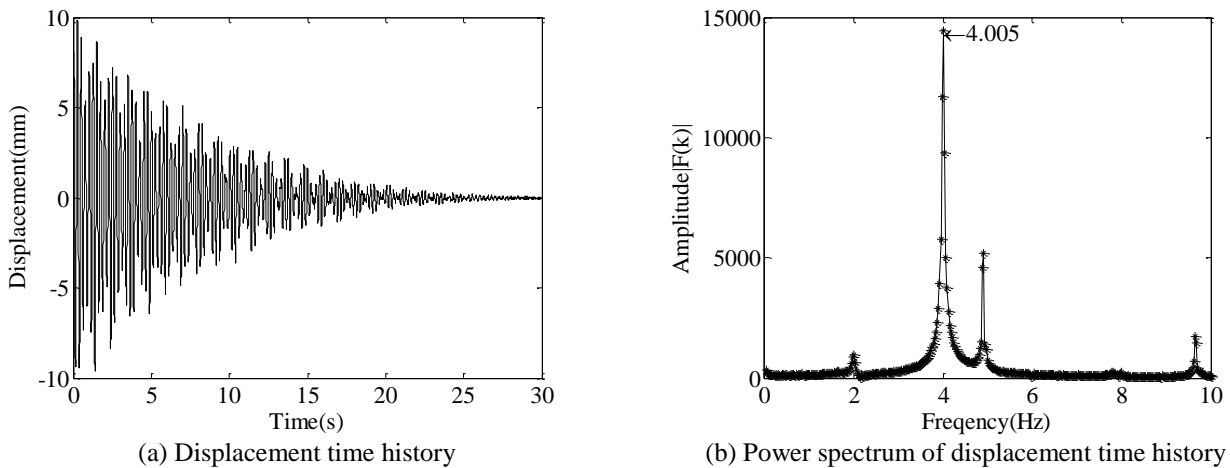


Fig. 9 First mode displacement time history and its power spectrum at mid-span of lower cable (cross-link located at  $0.2L$  and  $\eta=0.54$ )

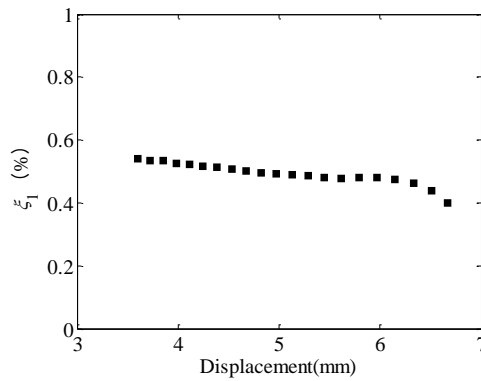


Fig. 10 First mode (first in-phase mode) damping ratio: mean  $\xi_1=0.4933\%$  (cross-link located at  $0.2L$  and  $\eta=0.54$ )

4.3 Test results

4.3.1 Single cable

Table 3 shows the 1<sup>st</sup> modal frequency and damping ratio of upper and lower model cables. It can be found that frequencies of the two tested cables were very close and the damping ratios were extremely low. The theoretical frequencies of the in-plane cable vibration were derived base on the following (Warnitchai 1990)

$$f_n = \frac{n}{2L} \sqrt{\frac{T}{m} \left[ 1 + \frac{2\chi^2}{n^4 \pi^4} (1 + (-1)^{n+1})^2 \right]} \quad (11)$$

where  $n$  is the vibration mode number, and the parameter

$$\chi^2 = \left( \frac{mgL}{T} \cos \theta \right)^2 \frac{LEA}{L_e T} \quad (\text{Irvine 1981}), \quad \text{in which}$$

$$L_e = L \left[ 1 + \left( \frac{mgL}{T} \cos \theta \right)^2 / 8 \right]$$

Table 3 1<sup>st</sup> mode frequency and damping ratio of two tested cables

Cables	Frequency(Hz)		Damping ratio (%)
	theoretical	test	
Upper cable	4.079	4.001	0.047
Lower cable	4.079	4.011	0.064

4.3.2 Twin-cables with a cross-link

Table 4 shows the 1<sup>st</sup> in-phase and out-of-phase mode frequency and damping ratio of the twin-cables with a cross-link but without oil damper. The cross-link was located from  $0.1L$  to  $0.5L$  with an interval of  $0.1L$ ; only half of cable length was tested due to symmetry. It clearly shows that the 1<sup>st</sup> in-phase mode frequency was slightly lower than that of single cable. The reason was the cross-link had no stiffness contribution for in-phase vibration. The added masses of clamping device and mental wire would decrease the vibration frequency (Zhou *et al.* 2018a), especially when mass was located at middle of the cable for 1<sup>st</sup> in-phase mode. However, the 1<sup>st</sup> out-of-phase mode frequency

Table 4 Frequency and damping ratio of 1<sup>st</sup> in-phase and out-of-phase modes of twin-cables with a cross-link

Cross-tie position	1 <sup>st</sup> in-phase		1 <sup>st</sup> out-of-phase	
	Damping ratio (%)	Frequency	Damping ratio (%)	Frequency
0.1L	0.119	3.987	0.210	4.379
0.2L	0.066	3.977	0.091	4.845
0.3L	0.141	3.993	0.214	5.559
0.4L	0.067	3.977	0.130	6.395
0.5L	0.203	3.958	0.150	7.680

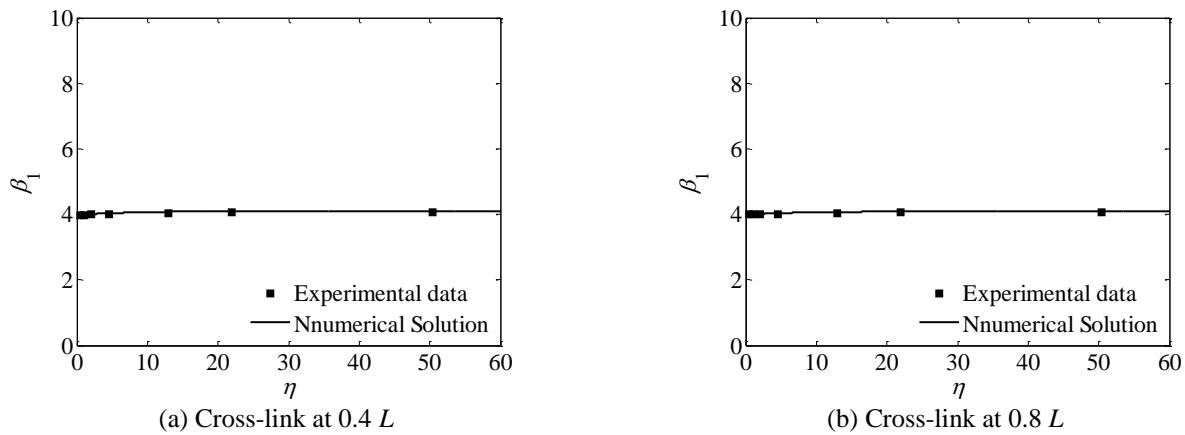


Fig. 11 First mode (first in-phase mode) frequency

was obviously larger than that of single cable for the out-of-phase vibration would stretch/compression the cross-link so it would contribute stiffness to the system. The damping ratios of the 1<sup>st</sup> in-phase and out-of-phase mode were also higher than that of single cable; however, it was still very low compared to the minimum damping ratio requirement for cable vibration mitigation (0.5%).

#### 4.3.3 Twin-cables with a cross-link and a viscous damper

The viscous damper was attached to the lower cable at 0.045L from the right cable end. The cross-link location is moved along upper cable axis at 0.1 L - 0.9 L from the right end of upper cable by an interval of 0.1 L. The effects of cross-link stiffness and damping coefficient on the in-phase and out-of-phase mode frequencies and damping ratios were discussed in the following.

Figs. 11 and 12 show the first mode (the first in-phase mode) and the second mode (the first out-of-phase mode) frequencies when the cross-link was located at 0.4 L and 0.8 L, respectively. It can be concluded that the in-phase mode frequency was very close to the numerical solution. In addition, the first mode frequency was also very close to the first mode frequency of single cable listed in Table 2 (4.001 Hz). The second mode frequency was about 1.6 times (cross-link located at 0.4L, frequency was about 6.4 Hz) and 1.25 times (cross-link located at 0.8L, frequency was about 5.0 Hz) to the single cable (4.001 Hz). In short, the cross-link didn't change the in-phase mode frequency, and could increase the out-of-phase mode frequency of the system.

Fig. 13 shows the first mode (first in-phase mode) damping ratio when the cross-link location was 0.2 L, 0.4 L, 0.6 L and 0.8 L from the right end of the upper cable. It could be observed that the system damping ratio was obviously larger than that of single cable. The damping ratio from the test (black squares) showed the same trend with the numerical results (black curves) as the system damping ratio increased at the beginning and reached to a maximum, then decreased as non-dimensional damping constant increasing. There was difference between the test damping ratio and the analytical damping ratio due to the effects of different factors. The test damping included the internal damping, and cross-ties would also increase the system damping a bit. The above factors may lead to larger test damping than analytical damping. However, there was also a detrimental factor that the tested damper coefficient was actually not the optimum one. There were also some factors that were hard to be evaluated, such as the measurement errors and the effects of environmental situations (indoor wind, environmental excitation, temperature variations, etc., although the effects of these factors were small in most situations). Anyway, the damping mechanism were actually very complex; the comparison results between the test damping to analytical damping were quite good as they were close in values and also showed similar changing pattern. The maximal damping ratio and the non-dimensional corresponding damping constant of the test result were also close to numerical ones. The approximate solutions from Eq. (7(a)) of Zhou *et al.* (2015) were also shown in Fig. 13 for

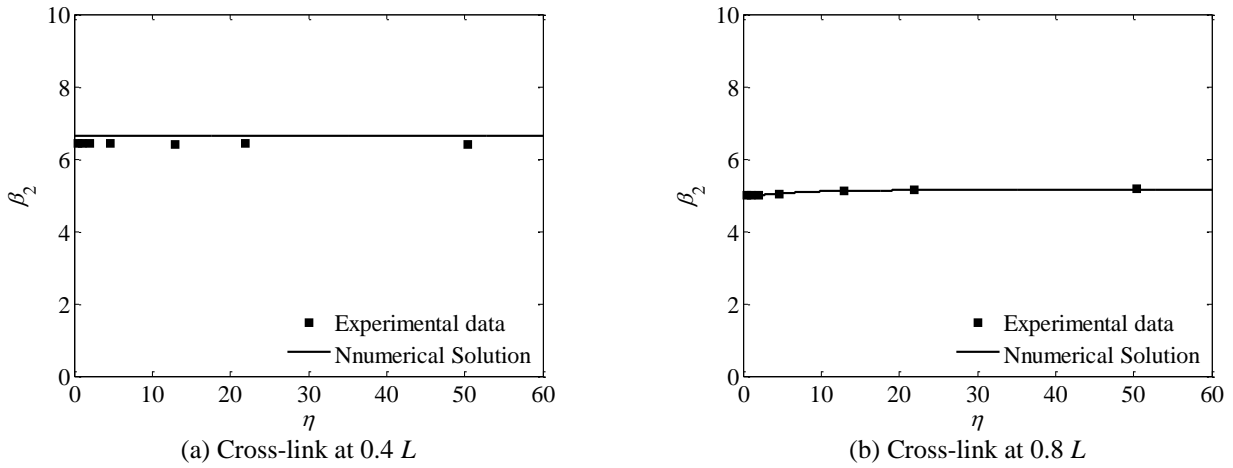


Fig. 12 Second mode (first out-of-phase mode) frequency

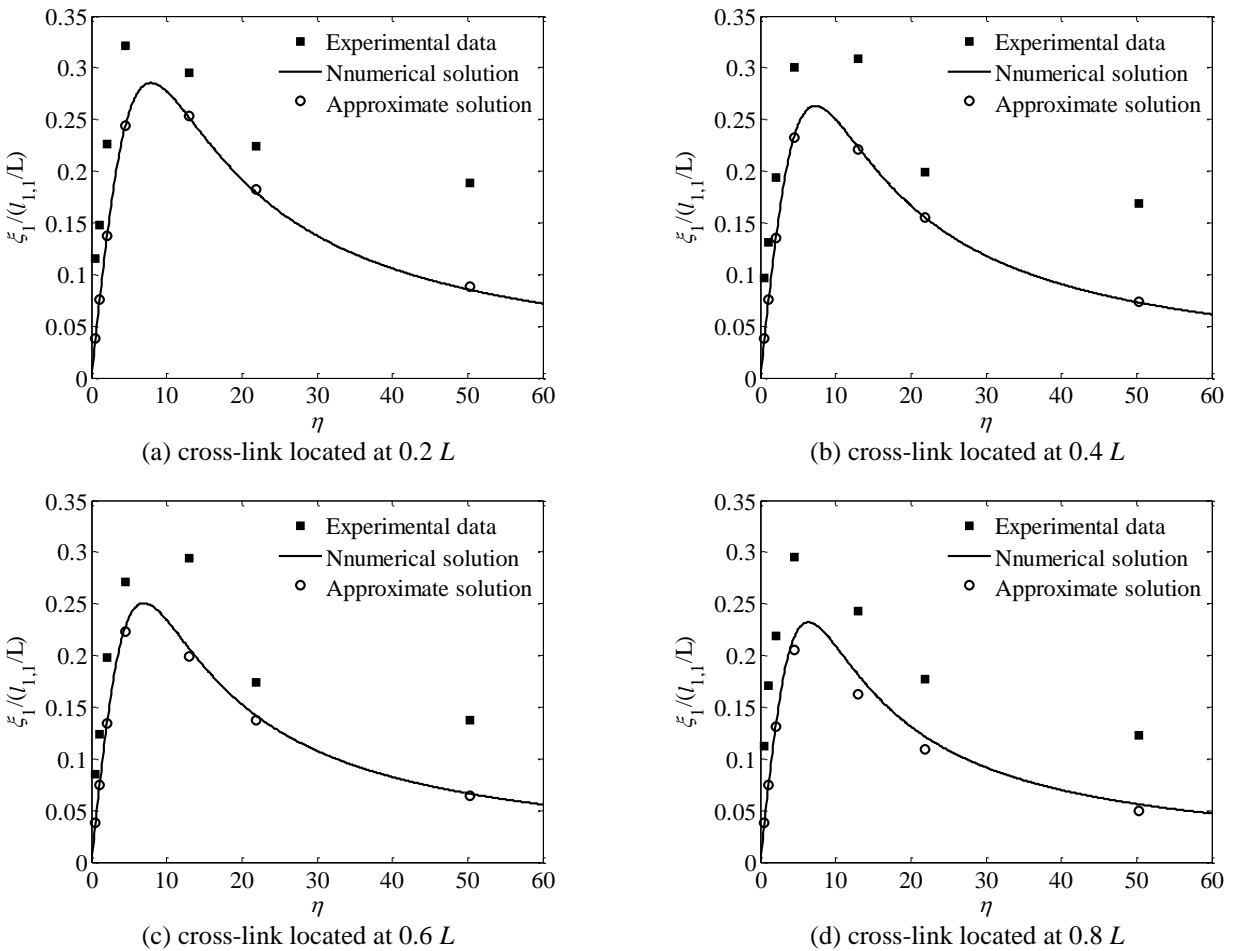


Fig. 13 First mode (first in-phase mode) damping ratio (damper located at  $l_{11}=0.045 L$ )

comparison, and it turned out that the approximate solution could well predict the system damping.

Fig. 14 shows the second mode (the first out-of-phase mode) damping ratio when the cross-link was located at  $0.6 L$ ,  $0.7 L$  and  $0.8 L$ . It can be concluded that the test result

also showed the same trend for the test and numerical results when cross-link was located at  $0.6 L$ ,  $0.7 L$  and  $0.8 L$ . The maximal damping ratio and the corresponding damping constant of test result were also close to numerical ones. The approximate solution from Eq. (7(b)) was also

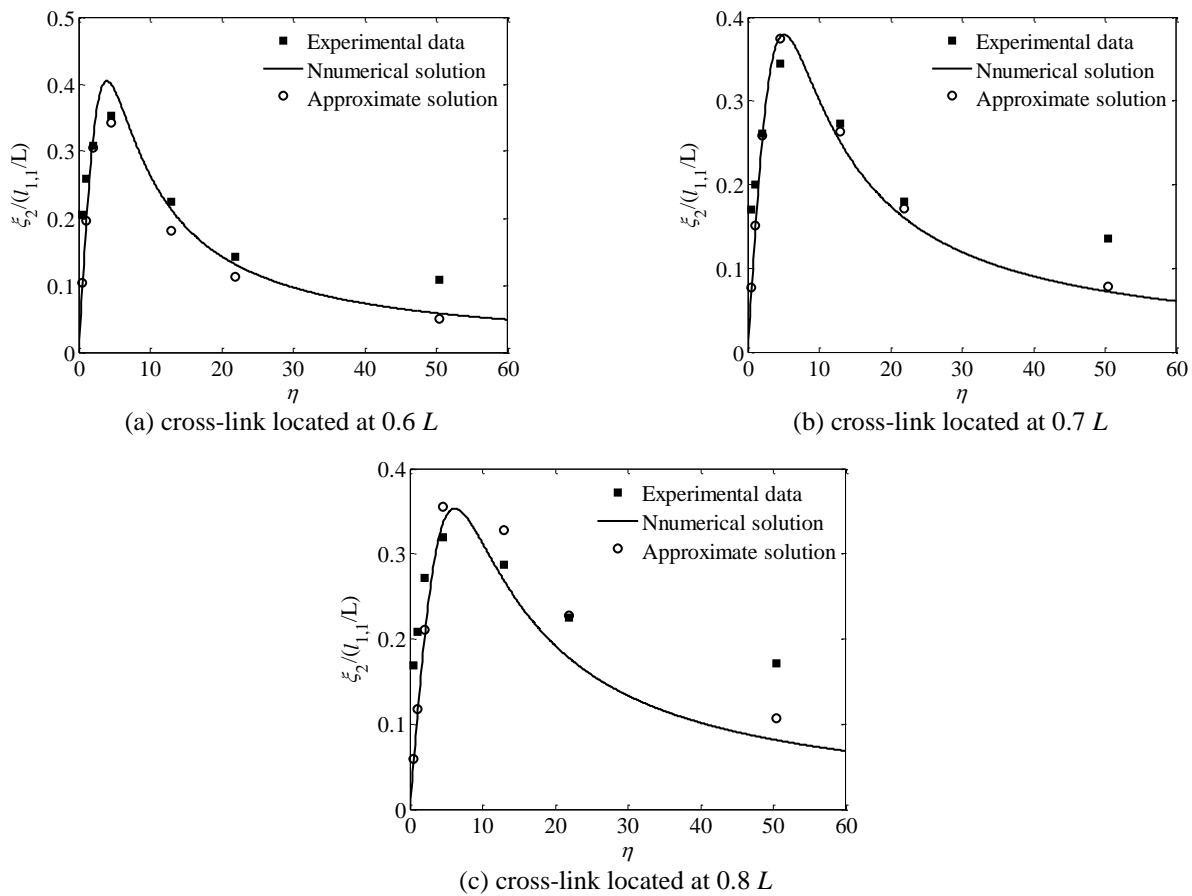


Fig. 14 Second mode (first out-of-phase mode) damping ratio (damper located at  $l_{d1}=0.045 L$ )

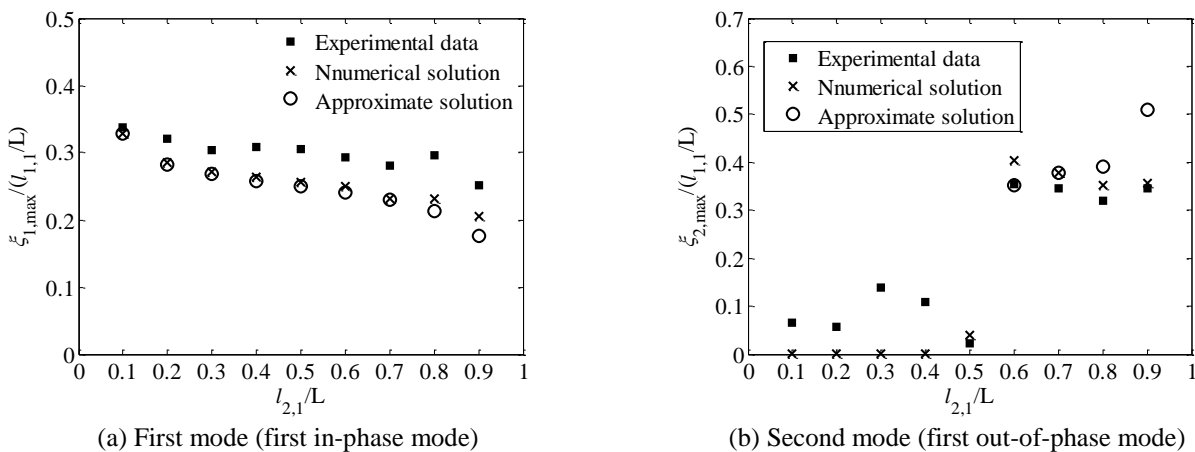


Fig. 15 Comparison of maximum damping ratio

shown in Fig. 14, it clearly showed that Eq. (7(b)) of Zhou *et al.* (2015) could well predict the test damping. When cross-link was located at  $0.4 L$ , the theoretical analysis showed that the damping ratio should be very small as the cable segment with attached damper would not vibrate; and the test result showed much smaller damping ratio as discussed in the following.

Fig. 15 further compares the maximum damping ratios of tested cases to that of the analytical solutions. Due to the fact of internal damping and the damper constant corresponding to the maximum damping ratio of the experiment was not the exact optimized damping constant, the experimental data was not exactly the same as the numerical ones. However, Fig. 15 still clearly shows that

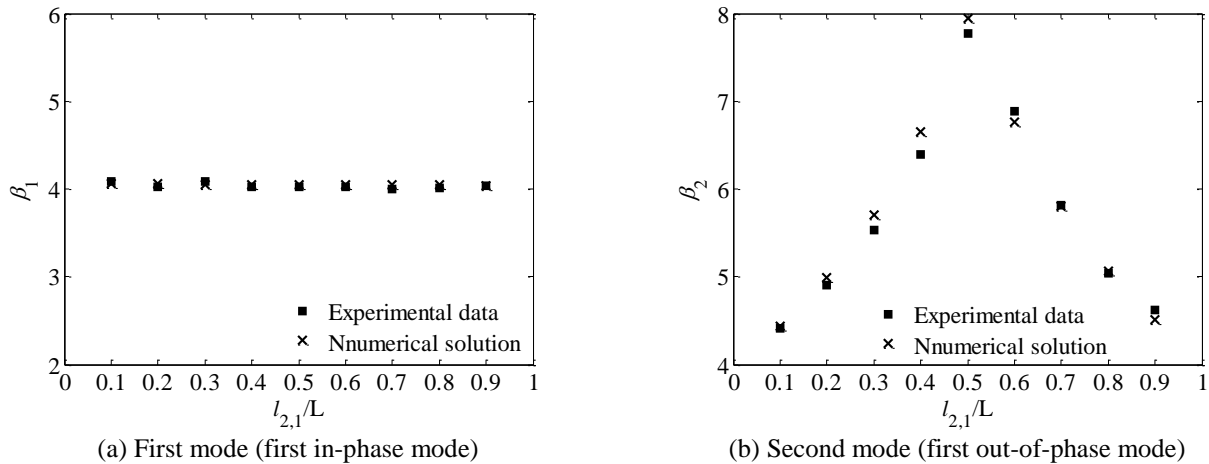


Fig. 16 Comparison of frequency corresponding to maximum damping ratio

the tested maximum damping ratios were very close to that of numerical solutions; especially the tested maximum damping ratios clearly showed the decreasing trend as the cross-link moved from the left to the right cable ends for the first in-phase mode. The approximate solutions (Eq. (8(a)) of Zhou *et al.* 2015) was also very close to that of numerical solutions. For the second mode vibration, the analytical study showed that the maximum damping ratio was very small (damper was in-effective) when the cross-link was located at  $0.1L$  to  $0.5L$ ; the test data confirmed this phenomenon for the damping was significantly smaller compared to that of other cross-link locations (Fig. 15(b)). The numerical maximum damping ratio was also very close to the tested when the cross-link was located at  $0.6L$  to  $0.9L$ . It should be noted that the approximate solution (Eq. (8(b)) of Zhou *et al.* 2015) could only predict the second mode maximum damping when cross-link was located at the half cable length far from the damper because it was assumed that the cable segment with attached damper would dominate the vibration of the system. The approximate maximum damping ratio was also close to that of numerical solution and test; however, the difference between the approximate maximum damping ratio and the numerical maximum damping ratio was large when the cross-link was located at  $0.9L$  due to the fact that  $l_{2,1}/L = 0.9$  and close to 1.

Fig. 16 shows the comparison of the frequencies, and the numerical results are also close to the test frequencies. All the above comparison showed that the analytical solutions could well predict the system behaviors.

## 5. Conclusions

This paper proposed a hybrid mitigation system of twin-cables by a connecting cross-tie and attaching a viscous damper; this kind of system could be referred to the vibration mitigation of hanger vibration by connecting two nearby hangers with a cross-tie and attaching one damper near to one hanger's end. The frequency equation of the

system was derived. Experimental studies were carried out. The tested system frequency and damping were further listed and compared to analytical solutions. The results are summarized as:

The system vibration mode still could be categorized by two solution branches: the in-phase mode and the out-of-phase mode as damper was near to cable end and had small effects on vibration frequency. The two solution branches showed different behaviors as the parameters of cross-link and damper changed.

For in-phase mode, one damper attachment can increase the maximum system damping ratio to almost half of the maximum damping ratio of a single cable with a damper. The cross-link stiffness and location had slight effects on the maximum damping ratio; and they have almost no effects on system frequency.

For out-of-phase mode, the maximum modal damping ratio is related to the cross-link location and stiffness. The maximum damping ratio can be close to zero or reach to the maximum damping ratio of a single cable attached with a damper when the cross-link moves along the cable axis. The cross-link location and stiffness have significant effects on system frequencies, especially when the cross-link is located at the antinode of single cable's mode shape.

The comparison showed that the analytical solution could well predict the test results: the tested damping and frequency were close to analytical ones. It was confirmed that the hybrid system had significantly higher damping for in-phase mode and higher frequency for out-of-phase mode compared to that of single free cable.

The above studies showed the damping and frequency could both be improved for the proposed hybrid system. It should be noted that connecting the two cables could also improve the vibration mass compared to that of single free cable. Further and on-going full-scale experiment or engineering applications will be carried out to improve and demonstrate the advantage of the proposed system in the near future.

## Acknowledgments

The authors of the work described in this paper received financial support from the National Natural Science Foundation of China (Grant Nos. 51578336 & 51108269), Shenzhen Knowledge Innovation Plan Project (Grant No. JCYJ20170818102511790) and the Ministry of Science and Technology for the 973-project (No. 2011CB013604), to whom the writers are grateful.

## References

- Ahmad, J. and Cheng, S.H. (2011), "Analytical study on in-phase modal properties of a general cable network", *Proceedings of the 9th International Symposium on Cable Dynamics*, Shanghai, China, October.
- Ahmad, J., Cheng, S.H. and Ghrib F. (2016), "Effect of the number of cross-tie lines on the in-plane stiffness and modal behavior classification of orthogonal cable networks with multiple lines of transverse flexible cross-ties", *J. Eng. Mech. - ASCE*, **142**(4), 04015106. [https://doi.org/10.1061/\(ASCE\)EM.1943-7889.0001008](https://doi.org/10.1061/(ASCE)EM.1943-7889.0001008).
- Bosch, H.R. and Park, S.W. (2005), "Effectiveness of external dampers and cross ties in mitigation of stay cable vibrations", *Proceedings of the 6th International Symposium on Cable Dynamics*, Charleston, USA, September.
- Caracoglia, L. and Jones, N.P. (2005), "In-phase dynamic behavior of cable networks. Part I: formulation and basic solutions", *J. Sound Vib.*, **279**(3-5), 969-991. <https://doi.org/10.1016/j.jsv.2003.11.058>.
- Caracoglia, L. and Jones, N.P. (2007), "Passive hybrid technique for the vibration mitigation of systems of interconnected stays", *J. Sound Vib.*, **307**(3-5), 849-864. <https://doi.org/10.1016/j.jsv.2007.07.022>.
- Caracoglia, L. and Zuo, D.L. (2009), "Effective of cable networks of various configurations in suppressing stay-cable vibration", *Eng. Struct.*, **31**(12), 2851-2864. <https://doi.org/10.1016/j.engstruct.2009.07.012>.
- Chen, Z.Q., Wang, X.Y., Ko, J.M., Ni, Y.Q., Spencer, B.F., Jr., Yang, G. and Hu, J.H. (2004), "MR damping system for mitigating wind-rain induced vibration on Dongting Lake Cable-Stayed Bridge", *Wind Struct.*, **7**(4), 293-304. <http://dx.doi.org/10.12989/was.2004.7.5.293>.
- Christenson, R.E., Spencer, B.F., Jr. and Johnson, E.A. (2006), "Experimental verification of smart cable damping", *J. Eng. Mech. - ASCE*, **132**(3), 268-278. [https://doi.org/10.1061/\(ASCE\)0733-9399\(2006\)132:3\(268\)](https://doi.org/10.1061/(ASCE)0733-9399(2006)132:3(268)).
- Duan Y.F., Ni Y.Q., H.M. Zhang, Spencer B.F., Jr. and Ko J.M. (2019a), "Design formulas for vibration control of taut cables using passive MR dampers", *Smart Struct. Syst.*, Accepted.
- Duan Y.F., Ni Y.Q., H.M. Zhang, Spencer B.F., Jr., and Ko J.M. (2019b), "Design formulas for vibration control of sagged cables using passive MR dampers", *Smart Struct. Syst.*, Accepted.
- Duan, Y.F., Ni, Y.Q. and Ko, J.M. (2005), "State-derivative feedback control of cable vibration using semi-active MR dampers", *Comput. -Aided Civil Infrastruct. Eng.*, **20**(6), 431-449. <https://doi.org/10.1111/j.1467-8667.2005.00396.x>.
- Duan, Y.F., Ni, Y.Q. and Ko, J.M. (2006), "Cable vibration control using magnetorheological dampers", *J. Intel. Mat. Syst. Str.*, **17**(4), 321-325.
- Fujino, Y. and Hoang, N. (2008), "Design formulas for damping of a stay cable with a damper", *J. Struct. Eng. - ASCE*, **134**(2), 269-278. [https://doi.org/10.1061/\(ASCE\)0733-9445\(2008\)134:2\(269\)](https://doi.org/10.1061/(ASCE)0733-9445(2008)134:2(269)).
- Gu, M. and Du, X.Q. (2005), "Testing investigation for rain-wind induced vibration and its mitigation", *J. Wind Eng. Ind. Aerod.*, **93**(1), 79-95.
- Gjelstrup, H., Georgikis, C. and Larsen, A. (2007), "A preliminary investigation of the hanger vibrations on the great belt east bridge", *Proceedings of the 7th International Symposium on Cable Dynamics*, Vienna, Austria, December.
- Hikami, Y. and Shiraishi, N. (1988), "Rain-wind induced vibration of cables in cable stayed bridges", *J. Wind Eng. Ind. Aerod.*, **29**(3), 409-418.
- Huang, L. (2011), "Experimental study on bridge stay cable vibration mitigation using external viscous damper", Master Thesis, University of Windsor, Windsor.
- Irvine H.M. (1981), *Cable Structures*. MIT Press, Cambridge, Massachusetts, 1981.
- Krenk, S. (2000), "Vibration of a taut cable with an external damper", *J. Appl. Mech.*, **67**(4), 772-776. [doi:10.1115/1.1322037](https://doi.org/10.1115/1.1322037).
- Krenk, S. and Hogsberg, J.R. (2005), "Damping of cables by a transverse force", *J. Eng. Mech. - ASCE*, **131**(4), 340-348. [https://doi.org/10.1061/\(ASCE\)0733-9399\(2005\)131:4\(340\)](https://doi.org/10.1061/(ASCE)0733-9399(2005)131:4(340)).
- Lu, L., Duan, Y.F., Spencer, B.F. Jr., Lu, X.L. and Zhou, Y. (2017), "Inertial mass damper for mitigating cable vibration", *Struct. Control Health Monit.*, e1986. <https://doi.org/10.1002/stc.1986>.
- Main, J.A. and Jones, N.P. (2001), "Evaluation of viscous dampers for stay-cable vibration mitigation", *J. Bridge Eng. - ASCE*, **6**(6), 385-397. [https://doi.org/10.1061/\(ASCE\)1084-0702\(2001\)6:6\(385\)](https://doi.org/10.1061/(ASCE)1084-0702(2001)6:6(385)).
- Main J.A. and Jones, N.P. (2002), "Free vibration of taut cable with attached damper, I: linear viscous damper", *J. Eng. Mech. - ASCE*, **128**(10), 1062-1071. [https://doi.org/10.1061/\(ASCE\)0733-9399\(2002\)128:10\(1062\)](https://doi.org/10.1061/(ASCE)0733-9399(2002)128:10(1062)).
- Or, S.W., Duan, Y.F., Ni, Y.Q., Chen, Z.H. and Lam, K.H. (2008). "Development of Magnetorheological dampers with embedded piezoelectric force sensors for structural vibration control", *J. Intel. Mat. Syst. Str.*, **19** (11), 1327-1338. <https://doi.org/10.1177/1045389X07085673>.
- Pacheco, B.M., Fujino, Y. and Sulekh, A. (1993), "Estimation curve for modal damping in stay cables with viscous damper", *J. Struct. Eng. - ASCE*, **119**(6), 1961-1979. [https://doi.org/10.1061/\(ASCE\)0733-9445\(1993\)119:6\(1961\)](https://doi.org/10.1061/(ASCE)0733-9445(1993)119:6(1961)).
- Shi, X., Zhu, S.Y., Li, J.Y. and Spencer, B.F. Jr. (2016), "Dynamic behavior of stay cables with passive negative stiffness dampers", *Smart Mater. Struct.*, **25**(7), 964-1726.
- Sun, L.M., Shi, C., Zhou, H.J. and Cheng, W. (2004), "A full-scale experiment on vibration mitigation of stay cable", *IABSE Symposium Report*, **88**(6), 31-36.
- Sun, L.M., Shi, C., Zhou, H.J. and Zhou, Y.G. (2005), "Vibration mitigation of long stay cable using dampers and cross-ties", *Proceedings of the 6th International Symposium on Cable Dynamics*, Charleston, SC, USA, September.
- Sun, L.M., Zhou, Y.G. and Huang, H.W. (2007), "Experiment and damping evaluation on stay cables connected by cross ties", *Proceedings of the 7th International Symposium on Cable Dynamics*, Vienna, Austria, December.
- Warnitchai, P. (1990), *Nonlinear vibration and active control of cable-stayed bridges*. PhD Thesis, University of Tokyo, Tokyo, Japan, 1990.
- Wang, X.Y., Ni, Y.Q., Ko, J.M. and Chen, Z.Q. (2005), "Optimal design of viscous dampers for multi-mode vibration control of bridge cables", *Eng. Struct.*, **27**(5), 792-800. <https://doi.org/10.1016/j.engstruct.2004.12.013>.
- Xu, Y.L., Chen, J., Ng, C.L. and Zhou, H.J. (2008), "Occurrence probability of wind-rain-induced stay cable vibration", *Adv. Struct. Eng.*, **11**(1), 53-69. <https://doi.org/10.1260/136943308784069487>.

- Yamaguchi, H. and Nagahawatta, H.D. (1995), "Damping effects of cable cross ties in cable-stayed bridges", *J. Wind Eng. Ind. Aerod.*, **54-55**, 35-43. [https://doi.org/10.1016/0167-6105\(94\)00027-B](https://doi.org/10.1016/0167-6105(94)00027-B).
- Zhan, S., Xu, Y.L. and Zhou, H.J. (2008), "Experimental study of wind-rain-induced cable vibration using a new model setup scheme", *J. Wind Eng. Ind. Aerod.*, **96**(12), 2348-2451. <https://doi.org/10.1016/j.jweia.2008.03.011>.
- Zhou, H.J., Huang X.J., Xiang N., He J.W., Sun, L.M. and Xing, F. (2018a), "Free vibration of a taut cable with a damper and a concentrated mass", *Struct. Control Health Monit.*, **25**(11), 1-21. <https://doi.org/10.1002/stc.2251>.
- Zhou, H.J., Qi, S.K., Yao, G.Z., Zhou, L.B., Sun, L.M. and Xing, F. (2018b), "Damping and frequency of a model cable attached with a pre-tensioned shape memory alloy wire: experiment and analysis", *Struct. Control Health Monit.*, **25**(2), 1-19. <https://doi.org/10.1002/stc.2106>.
- Zhou, H.J. and Sun, L.M. (2008), "Parameter optimization of damper with stiffness for stay cable", *Chinese Quarterly of Mechanics*, **29**(1), 180-185. (In Chinese)
- Zhou, H.J. and Sun, L.M. (2013), "Damping of stay cable with passive-on magnetorheological dampers: a full-scale test", *Int. J. Civil Eng.*, **11**(3), 154-159.
- Zhou, H.J., Sun, L.M. and Xing, F. (2014a), "Free vibration of taut cable with a damper and spring", *Struct. Control Health Monit.*, **21**(6), 996-1014. <https://doi.org/10.1002/stc.1628>.
- Zhou, H.J., Sun, L.M. and Xing, F. (2014b), "Damping of full-scale stay cable with viscous damper: experiment and analysis", *Adv. Struct. Eng.*, **17**(2), 265-274. <https://doi.org/10.1260/1369-4332.17.2.265>.
- Zhou, H.J., Sun, L.M. and Shi, C. (2006), "A full-scale experimental study on cable vibration mitigation with friction damper", *J. Tongji University*, **34**(7), 864-868. (In Chinese)
- Zhou, H.J., Xiang N., Huang X.J., Sun, L.M., Xing, F. and Zhou R. (2018c), "Full-scale test of dampers for stay cable vibration mitigation and improvement measures", *Struct. Monit. Maint.*, **5**(4), 489-506. <https://doi.org/10.12989/smm.2018.5.4.489>.
- Zhou, H.J., Yang, X., Sun, L.M. and Xing, F. (2015), "Free vibrations of a two-cable network with near-support dampers and a cross-link", *Struct. Control Health Monit.*, **22**(9), 1173-1192. <https://doi.org/10.1002/stc.1738>.
- Zhou, H.J., Wu, Y.H., Li, L.X., Sun, L.M. and Xing, F. (2019), "Free vibrations of a two-cable network inter-supported by cross-links extended to ground", *Smart Struct. Syst.*, Accepted.
- Zhou, P. and Li, H. (2016), "Modeling and control performance of a negative stiffness damper for suppressing stay cable vibrations", *Struct. Control Health Monit.*, **23**(4), 764-782. <https://doi.org/10.1002/stc.1809>.